

Is There an Optimal ENSO Pattern That Enhances Large-Scale Atmospheric Processes Conducive to Tornado Outbreaks in the United States?

SANG-KI LEE

Cooperative Institute for Marine and Atmospheric Studies, University of Miami, and Atlantic Oceanographic and Meteorological Laboratory, NOAA, Miami, Florida

ROBERT ATLAS

Atlantic Oceanographic and Meteorological Laboratory, NOAA, Miami, Florida

DAVID ENFIELD

Cooperative Institute for Marine and Atmospheric Studies, University of Miami, and Atlantic Oceanographic and Meteorological Laboratory, NOAA, Miami, Florida

CHUNZAI WANG

Atlantic Oceanographic and Meteorological Laboratory, NOAA, Miami, Florida

HAILONG LIU

Cooperative Institute for Marine and Atmospheric Studies, University of Miami, and Atlantic Oceanographic and Meteorological Laboratory, NOAA, Miami, Florida

(Manuscript received 5 March 2012, in final form 3 June 2012)

ABSTRACT

The record-breaking U.S. tornado outbreaks in the spring of 2011 prompt the need to identify long-term climate signals that could potentially provide seasonal predictability for U.S. tornado outbreaks. This study uses both observations and model experiments to show that a positive phase TransNiño may be one such climate signal. Among the top 10 extreme outbreak years during 1950–2010, seven years including the top three are identified with a strongly positive phase TransNiño. The number of intense tornadoes in April–May is nearly doubled during the top 10 positive TransNiño years from that during 10 neutral years. TransNiño represents the evolution of tropical Pacific sea surface temperatures (SSTs) during the onset or decay phase of the El Niño–Southern Oscillation. A positive phase TransNiño is characterized by colder than normal SSTs in the central tropical Pacific and warmer than normal SSTs in the eastern tropical Pacific. Modeling experiments suggest that warmer than normal SSTs in the eastern tropical Pacific work constructively with colder than normal SSTs in the central tropical Pacific to force a strong and persistent teleconnection pattern that increases both the upper-level westerly and lower-level southwesterly over the central and eastern United States. These anomalous winds advect more cold and dry upper-level air from the high latitudes and more warm and moist lower-level air from the Gulf of Mexico converging into the east of the Rockies, and also increase both the lower-tropospheric (0–6 km) and lower-level (0–1 km) vertical wind shear values therein, thus providing large-scale atmospheric conditions conducive to intense tornado outbreaks over the United States.

Corresponding author address: Dr. Sang-Ki Lee, NOAA/AOML, 4301 Rickenbacker Causeway, Miami, FL 33149.
E-mail: sang-ki.lee@noaa.gov

DOI: 10.1175/JCLI-D-12-00128.1

© 2013 American Meteorological Society

1. Introduction

In April and May of 2011, a record-breaking 1084 tornadoes and 541 tornado-related fatalities were confirmed in the United States, making 2011 one of the deadliest tornado years in U.S. history (<http://www.spc.noaa.gov/climo/online/monthly/newm.html#2011>). Questions were raised almost immediately as to whether the series of extreme tornado outbreaks in 2011 could be linked to long-term climate variability. The Severe Weather Database (SWD) from the National Oceanic and Atmospheric Administration (NOAA) indicates that the number of total U.S. tornadoes (i.e., from F0 to F5 in the Fujita–Pearson scale) during the most active tornado months of April and May (AM) has been steadily increasing since 1950 (Fig. 1). However, because of well-known inhomogeneity in the SWD over time associated with improvements in tornado detection technology, increased eyewitness reports due to population increase, and changes in damage survey procedures, one must be cautious in attributing this secular increase in the number of U.S. tornadoes to a specific long-term climate signal (Brooks and Doswell 2001; Verbout et al. 2006). In this study, only intense U.S. tornadoes (i.e., from F3 to F5 on the Fujita–Pearson scale) are selected and used since intense and long-track tornadoes are less likely to be affected by—although they are not completely free from—the known issues in the tornado database.

In the United States east of the Rocky Mountains, cold and dry upper-level air from the high latitudes often converges with warm and moist lower-level air coming from the Gulf of Mexico (GoM). Because of this so-called large-scale differential advection—i.e., any vertical variation of the horizontal advection of heat and moisture that decreases the vertical stability of the air column (Whitney and Miller 1956)—a conditionally unstable atmosphere with high convective available potential energy is formed. The lower-tropospheric [$\sim(0\text{--}6)$ km] vertical wind shear associated with the upper-level westerly and lower-level southwesterly winds (i.e., wind speed increasing and/or wind direction changing with height) provides the rotation with respect to a horizontal axis. The axis of this horizontal vortex tube can be tilted to the vertical by updrafts and downdrafts to form an intense rotating thunderstorm known as a supercell, which is the storm type most apt to spawn intense tornadoes (Lemon and Doswell 1979; Doswell and Bosart 2001). Increased low-level [$\sim(0\text{--}1)$ km] vertical wind shear is an additional atmospheric condition that distinguishes tornadic supercells from nontornadic supercells. Consistently, the moisture transport from the GoM to the United States and both the lower-tropospheric and lower-level vertical wind shear values in the central and

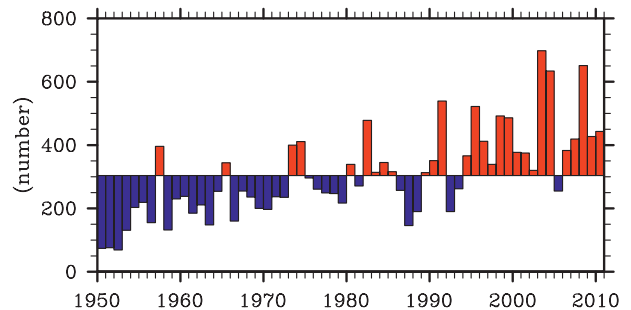


FIG. 1. The number of all (F0–F5) U.S. tornadoes for the most active tornado months of April and May (AM) during 1950–2010 obtained from SWD.

eastern United States are positively correlated with the number of intense U.S. tornadoes in AM (Table 1).

The Pacific–North American (PNA) pattern in boreal winter and spring is linked to the large-scale differential advection and the lower-tropospheric vertical wind shear in the central and eastern United States (Horel and Wallace 1981; Wallace and Gutzler 1981; Barnston and Livezey 1987). During a negative phase of the PNA, an anomalous upper-level cyclone is formed over North America that shifts the jet stream (and also the mid-latitude storm tracks) northward, thus advecting more cold and dry upper-level air to the central and eastern United States, and an anomalous anticyclone is formed over the southeastern seaboard that increases the southwesterly wind from the GoM to the United States, thus enhancing the Gulf-to-U.S. moisture transport. The upper-level cyclone also contributes to the development of steep lapse rates and removal of convective inhibition in the region of strong rising motion downstream from the cyclone (due to differential vorticity advection) and thus sets up a favorable environment for tornadogenesis (e.g., Doswell and Bosart 2001). Additionally, the lower-tropospheric vertical wind shear is increased over the central and eastern United States during a negative phase of the PNA due to the increased upper-level westerly and lower-level southwesterly flow.

Although the PNA is a naturally occurring atmospheric phenomenon driven by intrinsic variability of the atmosphere, a La Niña in the tropical Pacific can project onto a negative phase PNA pattern (Lau and Lim 1984; Straus and Shukla 2002). In addition, since the Gulf-to-U.S. moisture transport can be enhanced with a warmer GoM, the sea surface temperature (SST) anomaly in the GoM can also affect U.S. tornado activity. During the decay phase of La Niña in spring, the GoM is typically warmer than usual (Alexander and Scott 2002). Therefore, the Gulf-to-U.S. moisture transport could be increased during the decay phase of La Niña in spring because of the increased SSTs in the GoM and the strengthening of the

TABLE 1. Correlation coefficients of various long-term climate patterns in December–February (DJF), February–April (FMA), and April and May (AM) with the number of intense tornadoes in AM during 1950–2010. The values in parenthesis are those with the intense U.S. tornado-days in AM during 1950–2010. All indices including the tornado index are detrended using a simple least squares linear regression. Correlation coefficients above the 95% significance based on a Student's t test are in bold. The ERSST3 and NCEP–NCAR reanalysis are used to obtain the long-term climate indices used in this table.

Index	DJF	FMA	AM
Gulf-to-U.S. moisture transport*	0.12 (0.09)	0.22 (0.10)	0.44 (0.34)
Lower-tropospheric (500–1000 hPa) wind shear	0.03 (0.04)	0.16 (0.14)	0.26 (0.23)
Lower-level (850–1000 hPa) wind shear	0.12 (0.09)	0.20 (0.12)	0.44 (0.35)
GoM SST	0.15 (0.15)	0.21 (0.16)	0.20 (0.19)
Niño-4	−0.22 (−0.19)	−0.20 (−0.18)	−0.19 (−0.18)
Niño-3.4	−0.13 (−0.11)	−0.13 (−0.12)	−0.11 (−0.11)
Niño-1 + 2	0.02 (0.03)	0.11 (0.11)	0.15 (0.13)
TNI	0.28 (0.26)	0.29 (0.28)	0.33 (0.29)
PNA	−0.05 (−0.02)	−0.10 (−0.06)	−0.20 (−0.16)
PDO	−0.12 (−0.09)	−0.10 (−0.11)	−0.14 (−0.20)
NAO	−0.01 (−0.07)	−0.10 (−0.14)	−0.18 (−0.18)

* The Gulf-to-U.S. moisture transport is obtained by averaging the vertically integrated moisture transport in the region of 30°–40°N, 100°–80°W. The wind shear terms are also averaged over the same region. The North Atlantic Oscillation (NAO) index and the Pacific–North American (PNA) pattern are defined as the first and second leading modes of rotated empirical orthogonal function analysis of monthly mean geopotential height at 500 hPa, respectively. The Pacific decadal oscillation (PDO) is the leading principal component of monthly SST anomalies in the North Pacific Ocean north of 20°N.

southwesterly wind from the GoM to the United States. Nevertheless, the connectivity between the El Niño–Southern Oscillation (ENSO) and U.S. tornado activity in AM is quite weak (Table 1), as reported in earlier studies (Marzban and Schaefer 2001; Cook and Schaefer 2008). Currently, seasonal forecast skill for intense U.S. tornado

outbreaks, such as occurred in 2011, has not been demonstrated.

Interestingly, among the long-term climate patterns considered in Table 1, the number of U.S. tornadoes in AM is more strongly correlated with the TransNiño (TNI) than any other climate pattern. The TNI, which is defined as the

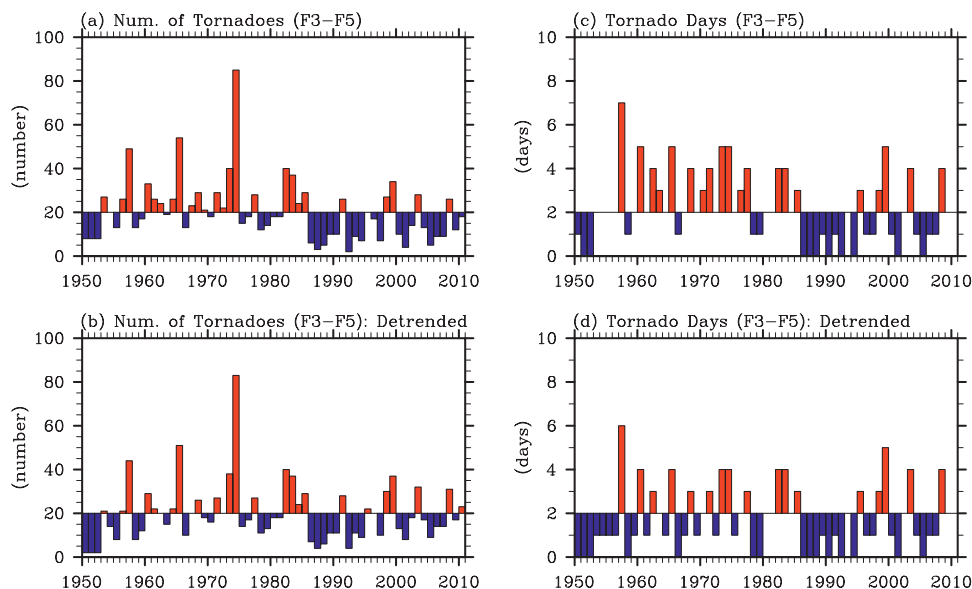


FIG. 2. (a) The number of intense (F3–F5) U.S. tornadoes and (c) the intense tornado-days for the most active tornado months of April and May (AM) during 1950–2010 obtained from SWD. The number of intense U.S. tornado-days is obtained by counting the number of days in which more than three intense tornadoes occurred. (b),(d) The detrended number of intense tornadoes and the detrended intense tornado-days, respectively.

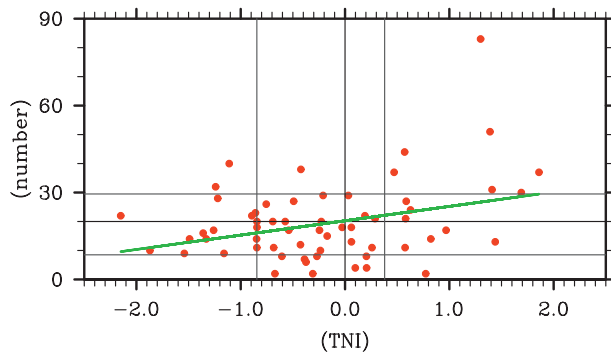


FIG. 3. Scatterplot of the TNI [computed from the extended reconstructed SST (ERSST3) dataset] vs the detrended number of intense U.S. tornadoes (obtained from SWD) in AM during 1950–2010. The green line shows the least squares regression fit with its slope ($\alpha = 4.96$) exceeding 99% confidence limit. The vertical lines to the left and right of the zero line show the lower and upper quartiles of the TNI index, respectively. The horizontal lines above and below the mean, separate normal activity years from the 10 most active and 10 least active years.

difference in normalized SST anomalies between the Niño-1 + 2 (10°S – 0° , 90° – 80°W) and Niño-4 (5°N – 5°S , 160°E – 150°W) regions, represents the evolution of ENSO in the months leading up to the event and the subsequent evolution with opposite sign after the event (Trenberth and Stepaniak 2001). Given that AM is typically characterized with the onset or decay phase of ENSO events, it is more likely that the tropical Pacific SST patterns in AM associated with ENSO are better represented by the TNI index than the conventional ENSO indices such as Niño-3.4 (5°N – 5°S , 170°W – 120°W) or Niño-3 (5°N – 5°S , 150° – 90°W). Nevertheless, it is not clear why U.S. tornado activity in AM is more strongly correlated with the TNI index than with other ENSO indices. This is the central question that we explore in the following sections by using both observations and an atmospheric general circulation model (AGCM).

2. U.S. tornado index

Since intense and long-track tornadoes are much more likely to be detected and reported even before a national network of Doppler radar was built in the 1990s, only the intense U.S. tornadoes in AM during 1950–2010 from the SWD are selected and used in this study. The number of intense U.S. tornadoes is used, after detrending, as the primary diagnostic index (Fig. 2b). Another tornado metric used in this study is “intense U.S. tornado-days” (Figs. 2c,d), which is obtained by counting the number of days in which more than a threshold number of intense tornadoes occurred (see Verboort et al. 2006). The threshold number selected in this case is 3 and above, which roughly represents the upper quartile in the number

TABLE 2. The 61 years from 1950 to 2010 are ranked based on the detrended number of intense U.S. tornadoes in AM. The top 10 extreme U.S. tornado outbreak years are listed with ENSO phase in spring and TNI index in AM for each year. Strongly positive (i.e., the upper quartile) and negative (i.e., the lower quartile) TNI index values are in bold and italic, respectively.

Ranking	Year	ENSO phase in spring	TNI index (detrended)
1	1974	La Niña persists	1.30 (1.48)
2	1965	La Niña transitions to El Niño	1.39 (1.54)
3	1957	La Niña transitions to El Niño	0.57 (0.69)
4	1982	El Niño develops	<i>-1.11 (-0.89)</i>
5	1973	El Niño transitions to La Niña	<i>-0.42 (-0.24)</i>
6	1999	La Niña persists	0.47 (0.75)
7	1983	El Niño decays	1.86 (2.08)
8	2003	El Niño decays	<i>-1.24 (-0.94)</i>
9	2008	La Niña decays	1.41 (1.73)
10	1998	El Niño transitions to La Niña	1.69 (1.97)

of intense U.S. tornadoes in a given day of AM during 1950–2010. In general, the tornado count index is sensitive to big tornado outbreak days, such as 3 April 1974 during which 60 intense tornadoes occurred over the United States. The tornado-days index, on the other hand, puts little weight on big tornado days. Since these two tornado indices are complementary to each other, it is beneficial to use both of these indices. The two tornado indices are further detrended by using a simple least squares linear regression.

3. Observed relationship between TNI and extreme U.S. tornado outbreaks

Table 1 shows that the TNI is significantly correlated with the number of intense tornadoes in AM. However, it is noted that the historical time series for the number of intense tornadoes is characterized by intense tornado outbreak years, such as 1974, 1965, and 1957, embedded among much weaker amplitude fluctuations (Figs. 2a,b). Therefore, the common practice of applying linear correlation (i.e., Pearson correlation) in this case is limited by the skewness (i.e., non-Gaussian distribution) in the tornado time series. This issue with the tornado time series can be seen more clearly in the scatterplot of the TNI versus the number of intense tornadoes in AM (Fig. 3). A simple way to remedy this data issue is to remove the most extreme year of 1974 and repeat the correlation test. In that case, the linear correlation between the TNI and the number of intense tornadoes falls to 0.25, which is barely significant at the 95% significance level based on a Student’s t test. Perhaps, a more formal alternative is to use ranking (or nonparametric) correlation methods, such as Kendall’s tau and Spearman’s rho, which are not sensitive to extreme years such as 1974.

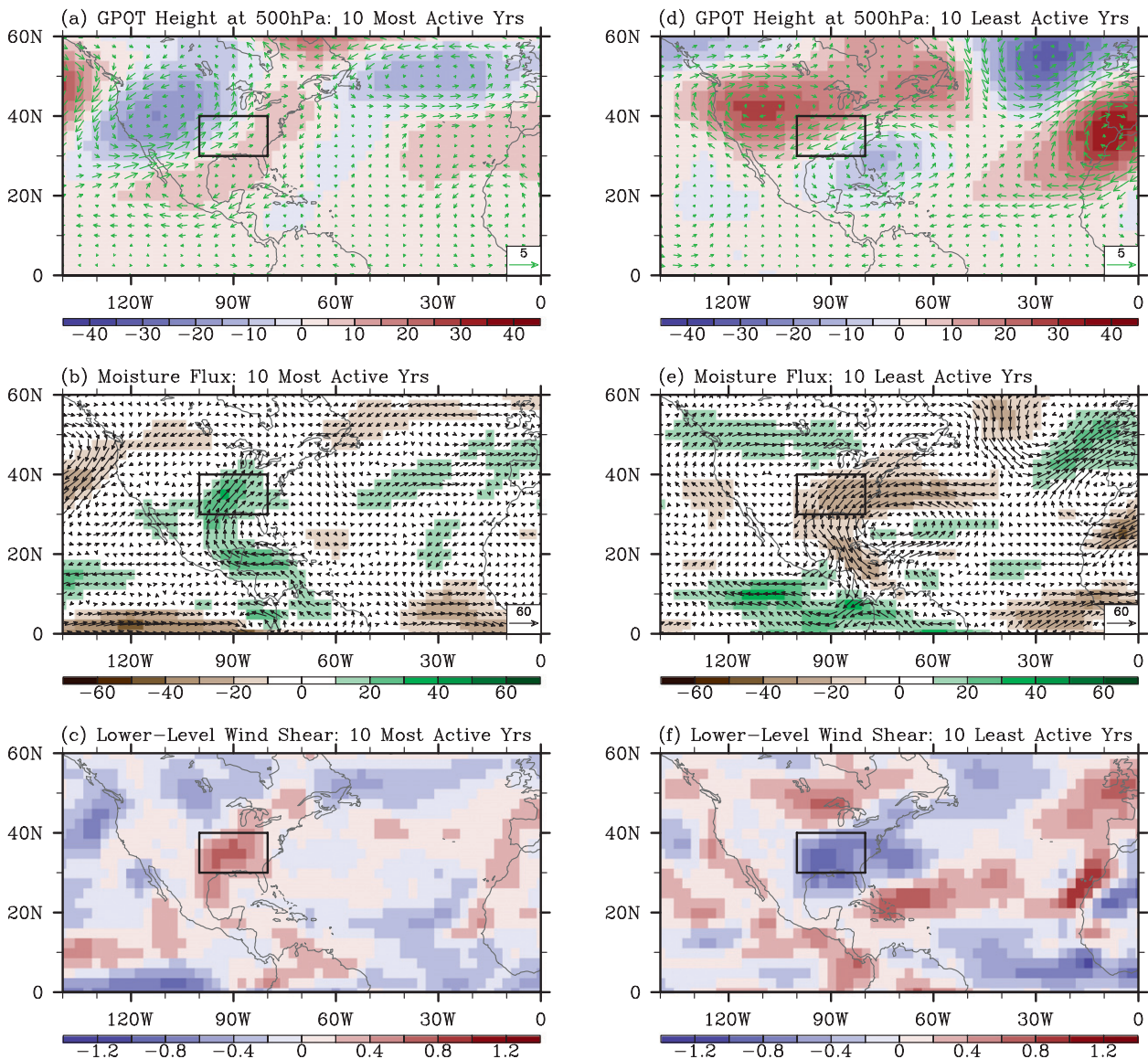


FIG. 4. (a),(d) Anomalous geopotential height and wind at 500 hPa, (b),(e) moisture transport, and (c),(f) lower-level (850–1000 hPa) vertical wind shear for the (left) 10 most active and (right) 10 least active U.S. tornado years in AM during 1950–2010 obtained from National Centers for Environmental Prediction (NCEP)–National Center for Atmospheric Research (NCAR) reanalysis. The units are $\text{kg m}^{-1} \text{s}^{-1}$ for moisture transport, m for geopotential height, and m s^{-1} for wind and wind shear. The small boxes indicate the central and eastern U.S. region frequently affected by intense tornadoes (30° – 40°N , 100° – 80°W). The values of the 90% confidence interval averaged over the box region are 15 (17) and 0.5 (0.4) for (b) [(e)] and (c) [(f)], respectively.

Ranking correlations basically replace the number of tornadoes in each year to its ranking among the 61-yr time series. Therefore, 1974 and 1965 will be given rankings of 1 and 2, respectively. Spearman's rho method is applied to find that the ranking correlation between the TNI and the number of intense tornadoes (intense tornado-days) falls to 0.16 (0.24), which is below (barely significant at) the 95% significance level, suggesting that the overall correlation between the TNI and the number of intense tornadoes is

not strong. Similarly, the TNI is only weakly correlated with tornadic environments (not shown).

However, it is important to note that the ranking correlation gives less weight to extreme outbreak years such as 1974, 1965, and 1957 and more weight to weak amplitude years, whereas the linear correlation is very sensitive to extreme years. What this means is that although the overall correlation between the TNI and the number of intense tornadoes is not strong, the TNI may be associated with

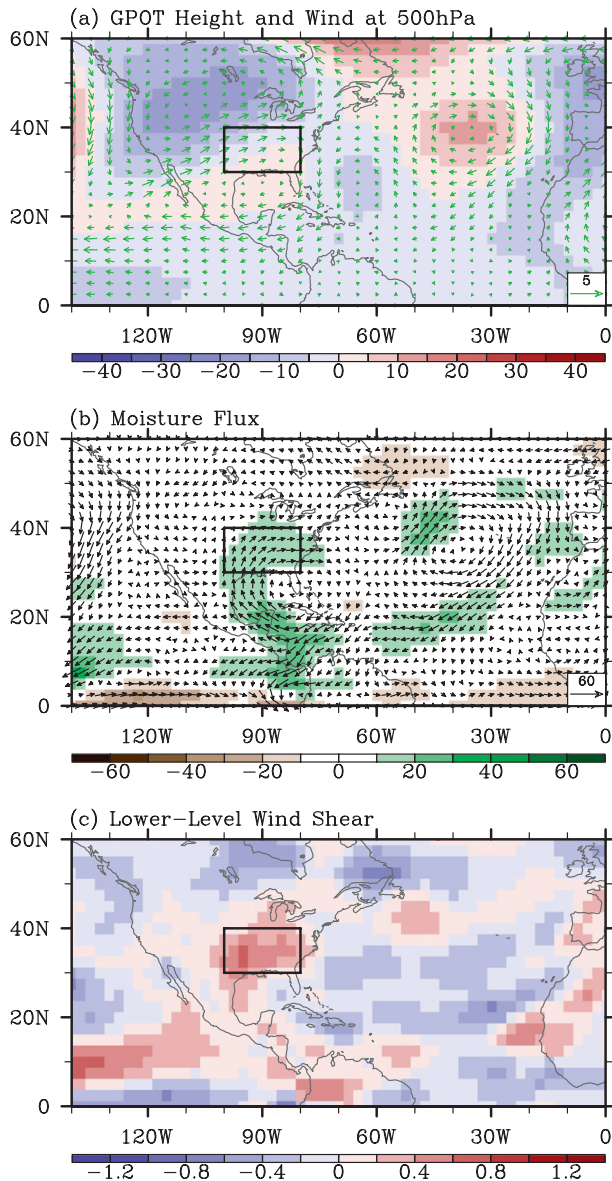


FIG. 5. As in Fig. 4, but for the top 10 positive TNI years. The values of the 90% confidence interval averaged over the box region are 16 and 0.5 for (b) and (c), respectively.

extreme outbreak years (see Fig. 3). Since the majority of tornado-related fatalities occur during those extreme outbreak years, here we focus our attention to those extreme years and associated large-scale atmospheric processes. Therefore, we first ranked the years from 1950 to 2010 (61 years in total) based on the number of intense U.S. tornadoes in AM. The top 10 extreme U.S. tornado outbreak years are listed in Table 2. Note that if the tornado ranking is redone based on the intense U.S. tornado-days in AM, 1998 in the top 10 list is replaced by 1960, but other top nine years remain in the top 10 (not shown).

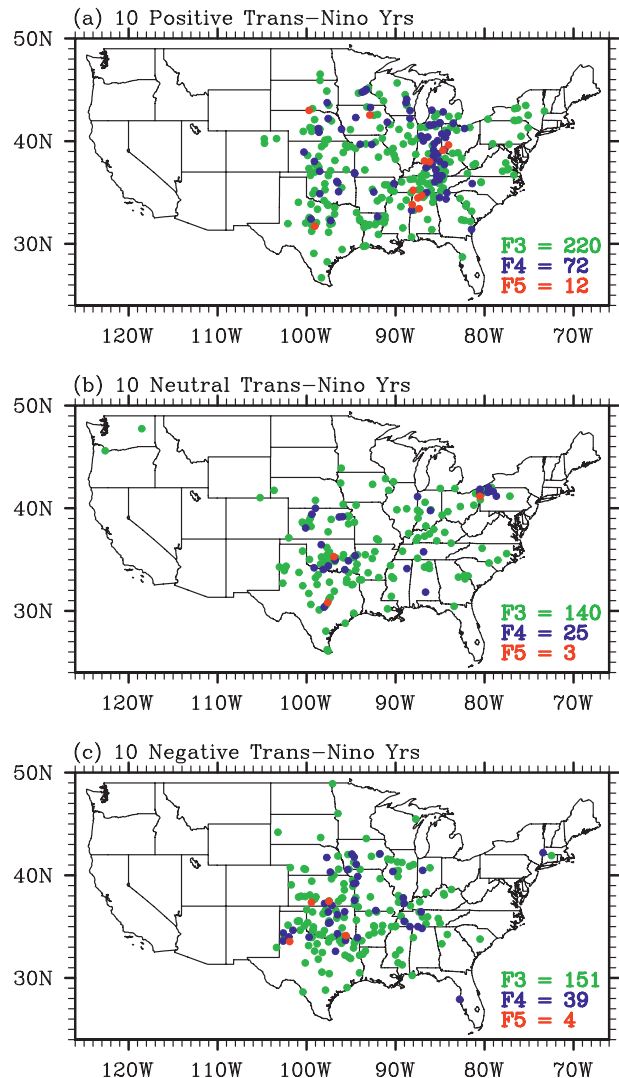


FIG. 6. Incidents of intense (F3–F5) U.S. tornadoes in AM for (a) the top 10 positive TNI years, (b) 10 neutral TNI years, and (c) the top 10 negative TNI years during 1950–2010 obtained from SWD. Green indicates F3, blue F4, and red F5 tornadoes.

The top 10 extreme tornado outbreak years are characterized by an anomalous upper-level cyclone over North America (Fig. 4a), increased Gulf-to-U.S. moisture transport (Fig. 4b), and increased lower-tropospheric (not shown) and lower-level vertical wind shear values over the east of the Rockies (Fig. 4c), whereas the bottom 10 years are associated with an anomalous upper-level anticyclone over North America (Fig. 4d), decreased Gulf-to-U.S. moisture transport (Fig. 4e), and decreased lower-tropospheric (not shown) and lower-level vertical wind shear values over the central and eastern United States (Fig. 4f). It is worthwhile to point out that all the composite maps and model results shown in this study

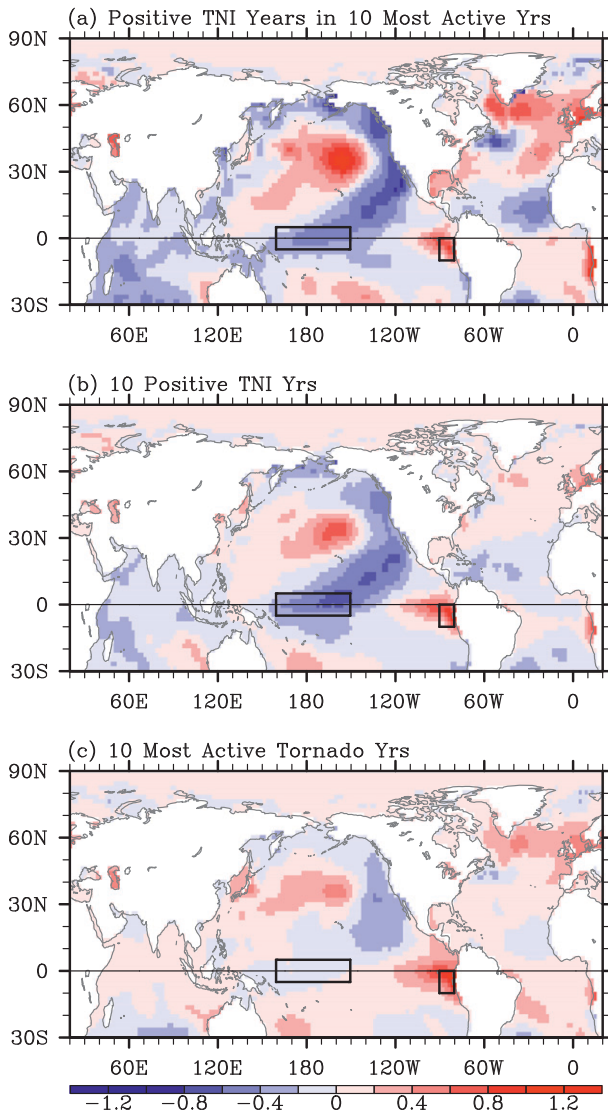


FIG. 7. Composite SST anomalies in AM, obtained from ERSST3 for (a) the 5 positive TNI years transitioning from a La Niña identified among the 10 most active U.S. tornado years in AM during 1950–2010, and for (b) the top 10 positive TNI years and (c) the 10 most active U.S. tornado years in AM during 1950–2010. Thick black rectangles indicate the Niño-4 (5°N – 5°S , 160°E – 150°W) and Niño-1 + 2 (10°S – 0° , 90° – 80°W) regions. The values of the 90% confidence interval averaged over the tropical Pacific (15°S – 15°N , 120°E –coast of the Americas) are 0.4, 0.3 and 0.3 for (a)–(c), respectively.

should be understood in a long-term averaged sense. For instance, the anomalous upper-level cyclone over North America shown in Fig. 4a is a long-term average over many days during which a series of cyclones as well as anticyclones may have passed over the area.

As in the top 10 extreme tornado outbreak years, the top 10 positive TNI (i.e., normalized SST anomalies are larger in the Niño-1 + 2 than in Niño-4 region) years are also characterized by an anomalous upper-level

TABLE 3. The 61 years from 1950 to 2010 are ranked based on the detrended number of intense U.S. tornadoes in AM. The bottom 10 years are listed with ENSO phase in spring and TNI index in AM for each year. Strongly positive (i.e., the upper quartile) and negative (i.e., the lower quartile) TNI index values are in bold and italic, respectively.

Ranking	Year	ENSO phase in spring	TNI index (detrended)
52	1958	El Niño decays	−0.61 (−0.49)
53	1955	La Niña persists	−0.27 (−0.16)
54	2001	La Niña decays	0.21 (0.50)
55	1986	El Niño develops	−0.39 (−0.16)
56	1988	El Niño transitions to La Niña	−0.37 (−0.13)
57	1987	El Niño persists	0.10 (0.34)
58	1992	El Niño decays	0.21 (0.47)
59	1952	Neutral	−0.67 (−0.57)
60	1951	La Niña transitions to El Niño	−0.31 (−0.22)
61	1950	La Niña persists	0.77 (0.86)

cyclone over North America (Fig. 5a), increased Gulf-to-U.S. moisture transport (Fig. 5b), and increased lower-tropospheric (not shown) and lower-level vertical wind shear values over the east of the Rockies (Fig. 5c). Because of these large-scale atmospheric conditions, the

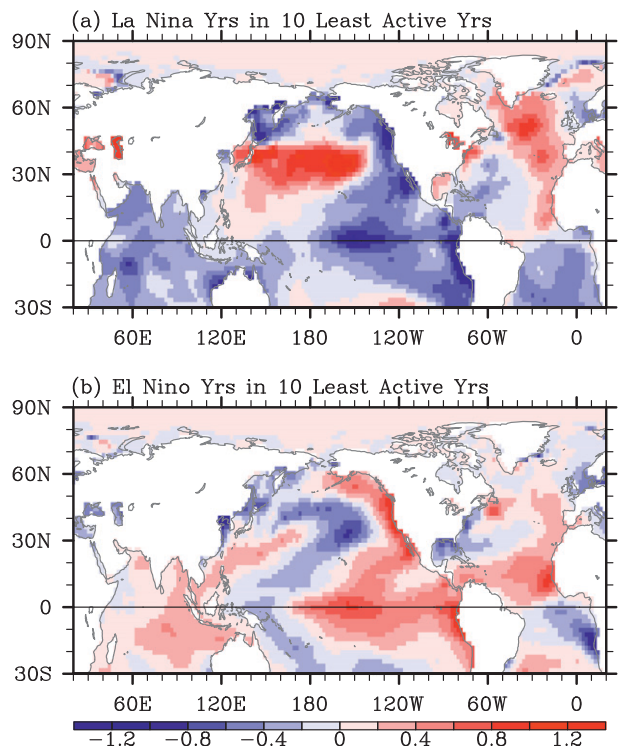


FIG. 8. Composite SST anomalies in AM obtained from ERSST3 for (a) the 4 years with a La Niña transitioning and (b) the 4 years with an El Niño transitioning identified among the 10 least active U.S. tornado years in AM during 1950–2010. The values of the 90% confidence interval averaged over the tropical Pacific (15°S – 15°N , 120°E –coast of the Americas) are 0.4 and 0.5 for (a) and (b), respectively.

TABLE 4. Prescribed SSTs in the tropical Pacific region for each model experiment. All model experiments are initiated in April of the prior year and continued to December of the modeling year. For instance, in EXP_TNI, the model is integrated for 21 months starting in April using the composite April SSTs of 1956, 1964, 1973, 1998, and 2007.

Experiments	Prescribed SSTs in the tropical Pacific region
EXP_CLM	Climatological SSTs are prescribed in the tropical Pacific region (15°S–15°N, 120°E–coast of the Americas).
EXP_TNI	Composite SSTs of the five positive phase TNI years transitioning from a La Niña identified among the 10 most active U.S. tornado years (1957, 1965, 1974, 1999, and 2008) are prescribed in the tropical Pacific region.
EXP_TN1	Same as EXP_TNI except that the composite SSTs of the top 10 positive TNI years are prescribed in the tropical Pacific region.
EXP_TN2	Same as EXP_TNI except that the composite SSTs of the top 10 most extreme tornado years are prescribed in the tropical Pacific region.
EXP_LAN	Composite SSTs of the four years with a La Niña transitioning (1950, 1951, 1955, and 2001) identified among the 10 least active U.S. tornado years are prescribed in the tropical Pacific region.
EXP_ELN	Composite SSTs of the four years with an El Niño transitioning (1958, 1987, 1988, and 1992) identified among the 10 least active U.S. tornado years are prescribed in the tropical Pacific region.
EXP_CPC	Same as EXP_TNI except that the composite SSTs are prescribed only in the western and central tropical Pacific region (15°S–15°N, 120°E–110°W), while in the eastern Pacific region (15°S–15°N, 110°W–coast of the Americas) climatological SSTs are prescribed.
EXP_EPW	Same as EXP_TNI except that the composite SSTs are prescribed only in the eastern tropical Pacific region (15°S–15°N, 110°W–coast of the Americas), while in the western and central tropical Pacific region (15°S–15°N, 120°E–110°W) climatological SSTs are prescribed.
EXP_011	SSTs for 2010–11 are prescribed in the tropical Pacific region.
EXP_WPW	Same as EXP_011 except that the SSTs for 2010–11 are prescribed only in the western Pacific region (15°S–15°N, 120°E–180°).

number of intense U.S. tornadoes in AM during the top 10 positive TNI years is nearly doubled from that during 10 neutral TNI years (Figs. 6a,b). Consistent with these findings, among the top 10 extreme tornado outbreak years, seven years including the top three are identified with a strongly positive phase (i.e., within the upper quartile) TNI as shown in Table 2 (also see Fig. 3). Five out of those seven years are characterized by a La Niña transitioning to a different phase or persisting beyond AM (1957, 1965, 1974, 1999, and 2008) and the other two with an El Niño transitioning to either a La Niña or neutral phase (1983 and 1998). The composite SST anomalies for those five positive phase TNI years transitioning from a La Niña are characterized by colder than normal SSTs in the central tropical Pacific (CP) and warmer than normal SSTs in the eastern tropical Pacific (EP) (Fig. 7a) as in the composite SST anomalies for the top 10 positive TNI years (Fig. 7b). If the top 10 extreme tornado outbreak years are averaged together, the composite SST anomalies are still characterized by a positive phase TNI (i.e., normalized SST anomalies are larger in the Niño-1 + 2 than in Niño-4 region), although the colder than normal SST anomalies in CP are nearly canceled out (Fig. 7c).

In the bottom 10 years, on the other hand, only one year is identified with a strongly positive phase TNI, and the other nine years are with a neutral phase TNI (i.e., between the lower and upper quartiles) as shown in Table 3 (also see Fig. 3). This result suggests that a negative phase

of the TNI does not decrease the number of intense U.S. tornadoes in AM, and thus partly explains why the overall correlation between the TNI and the number of intense U.S. tornadoes in AM is not high. Consistently, the number of intense U.S. tornadoes in AM during the top 10 negative phase TNI years is not much changed from that during 10 neutral phase TNI years (Figs. 6b,c). Interestingly, four years among the bottom 10 years are identified with a La Niña transitioning to a different phase or persisting beyond AM (1950, 1951, 1955, and 2001), and four are identified with an El Niño transitioning to a different phase or persisting beyond AM (1958, 1987, 1988, and 1992). The composite SST anomaly pattern for the four years of the bottom 10 years with a La Niña transitioning is that of a typical La Niña with the SST anomalies in the Niño-4 and Niño-1 + 2 being both strongly negative (i.e., neutral phase TNI) (Fig. 8a). Similarly, the composite SST anomaly pattern for the four years in the bottom 10 years with an El Niño transitioning is that of a typical El Niño with the SST anomalies in the Niño-4 and Niño-1 + 2 being both strongly positive (i.e., neutral phase TNI) (Fig. 8b).

In summary, observations seem to indicate that a positive phase of the TNI (i.e., normalized SST anomalies are larger in the Niño-1 + 2 than in Niño-4 region) is linked to extreme U.S. tornado outbreaks in AM, whereas either La Niñas and El Niños with a neutral phase TNI (i.e., the SST anomalies in the Niño-1 + 2 region are as strong and the same sign as the SST anomalies in the Niño-4) are not linked to extreme U.S. tornado outbreaks in AM.

4. Model experiments

To explore the potential link between the tropical Pacific SST anomaly patterns, identified in the previous section (Figs. 7 and 8), and the number of intense U.S. tornadoes in AM, a series of AGCM experiments are performed by using version 3.1 of the National Center for Atmospheric Research Community Atmospheric Model version 3 (CAM3) coupled to a slab mixed layer ocean model. The model is a global spectral model with a triangular spectral truncation of the spherical harmonics at zonal wavenumber 42. It is vertically divided into 26 hybrid sigma-pressure layers. Model experiments are performed by prescribing various composite evolutions of SSTs in the tropical Pacific region (15°S – 15°N , 120°E –coast of the Americas) while predicting the SSTs outside the tropical Pacific using the slab ocean model. To prevent discontinuity of SST around the edges of the forcing region, the model SSTs of three grid points centered at the boundary are determined by combining the simulated and prescribed SSTs. Each ensemble consists of 10 model integrations that are initialized with slightly different conditions to represent intrinsic atmospheric variability. The same methodology was previously used for studying ENSO teleconnection to the tropical North Atlantic region (Lee et al. 2008, 2010).

Six sets of ensemble runs are performed (Table 4). In the first experiment (EXP_CLM), the SSTs in the tropical Pacific region are prescribed with climatological SSTs. In the second experiment (EXP_TNI), the composite SSTs of the positive phase TNI years identified among the 10 most active U.S. tornado years are prescribed in the tropical Pacific region. Note that only the five positive TNI years transitioning from a La Niña are considered in this case (Fig. 7a). Two experiments similar to EXP_TNI are carried out by prescribing the SSTs in the tropical Pacific region with the composite SSTs of the top 10 positive TNI years (Fig. 7b) for EXP_TN1 and the top 10 most extreme tornado years (Fig. 7c) for EXP_TN2. In the next two experiments, the SSTs in the tropical Pacific region are prescribed with the composite SSTs of the four years in the bottom 10 years with a La Niña transitioning (Fig. 8a) for EXP_LAN, and the four years in the bottom 10 years with an El Niño transitioning (Fig. 8b) for EXP_ELN.

5. Simulated impact of TNI on tornadic environments

In EXP_TNI (Fig. 9), an anomalous upper-level cyclone is formed over North America that shifts the jet stream northward, thus advecting more cold and dry

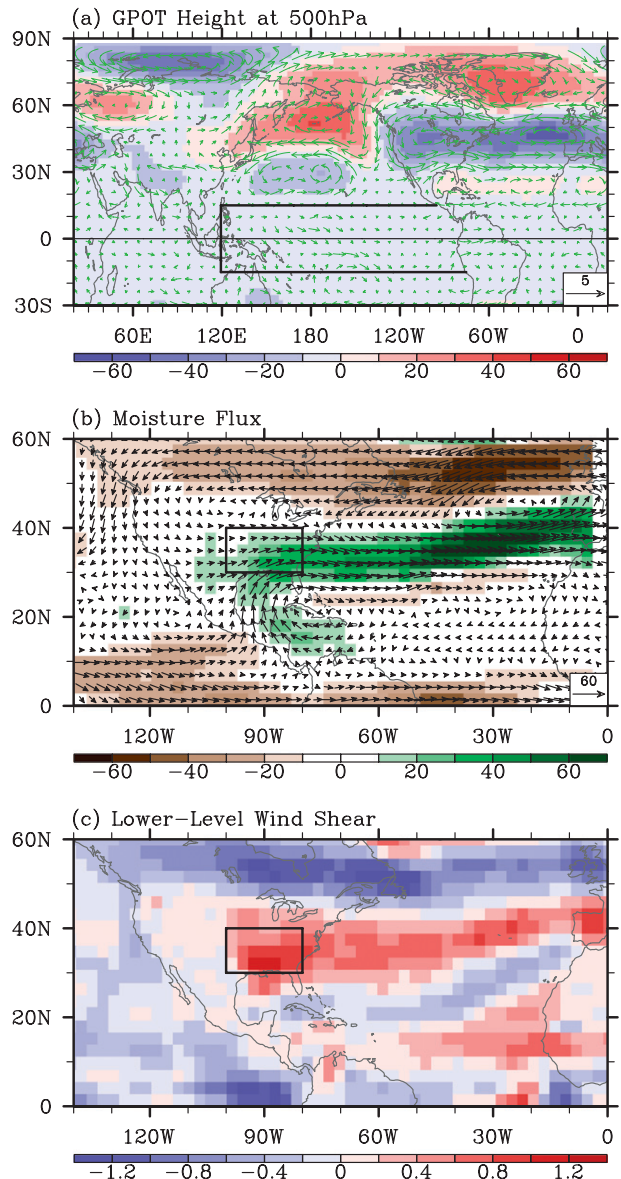


FIG. 9. Simulated anomalous (a) geopotential height and wind at 500 hPa, (b) moisture transport, and (c) lower-level (850–1000 hPa) vertical wind shear in AM obtained from EXP_TNI – EXP_CLM. The units are $\text{kg m}^{-1} \text{s}^{-1}$ for moisture transport, m for geopotential height, and m s^{-1} for wind and wind shear. Thick black lines in (a) indicate the tropical Pacific region where the model SSTs are prescribed. The small boxes in (b) and (c) indicate the central and eastern U.S. region frequently affected by intense tornadoes (30° – 40°N , 100° – 80°W). The values of the 90% confidence interval averaged over the box region are 17 and 0.5 for (b) and (c), respectively.

upper-level air to the central and eastern U.S. The Gulf-to-U.S. moisture transport and the lower-tropospheric (not shown) and lower-level vertical wind shear values are increased over the central and eastern United States. All of these are large-scale atmospheric conditions conducive

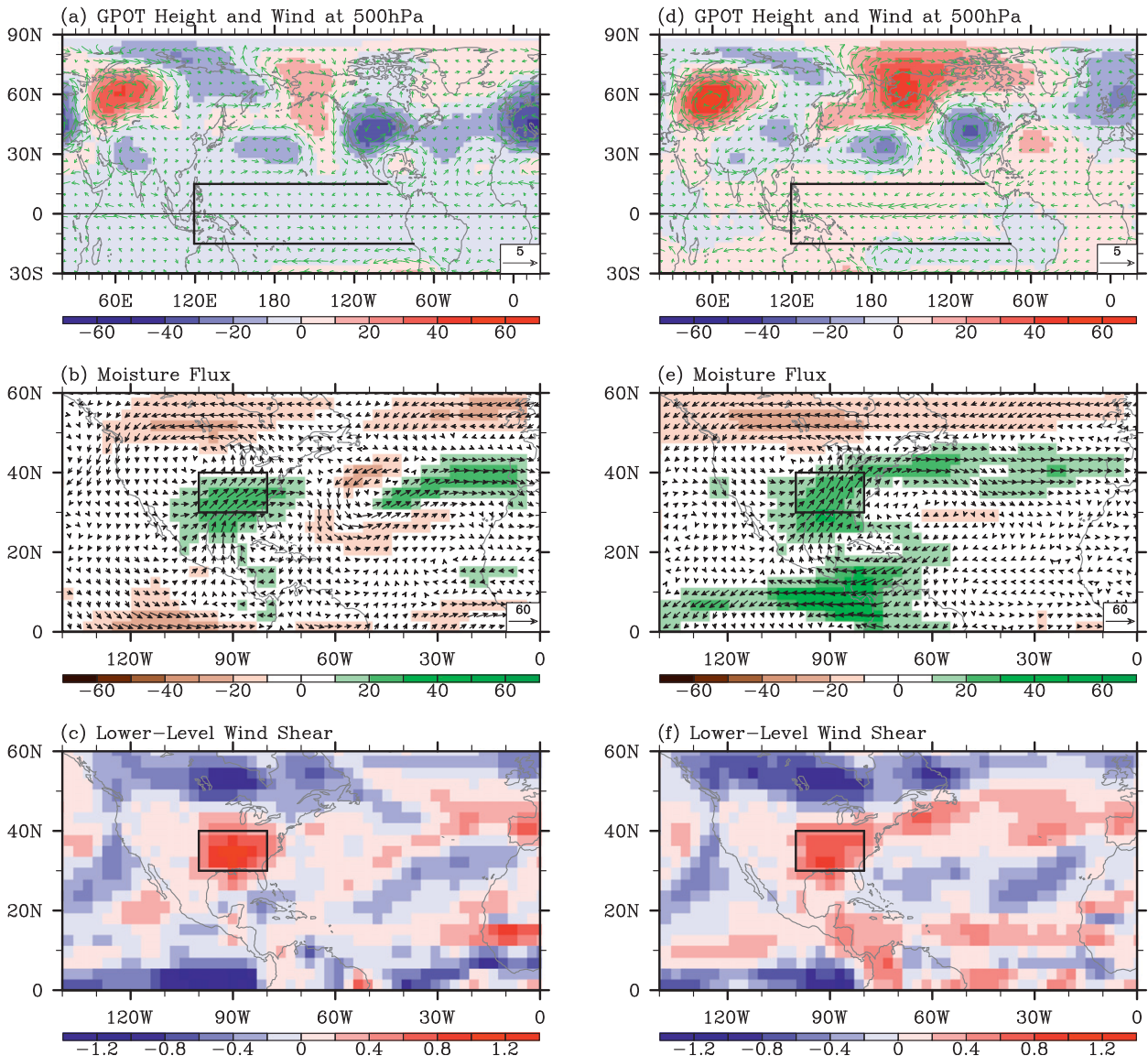


FIG. 10. As in Fig. 9, but obtained from (a)–(c) EXP_TN1 – EXP_CLM and (d)–(f) EXP_TN2 – EXP_CLM. The values of the 90% confidence interval averaged over the box region are 23 (26) and 0.4 (0.6) for (b) [(e)] and (c) [(f)], respectively.

to intense tornado outbreaks over the United States and they are also well reproduced in both EXP_TN1 and EXP_TN2 (Fig. 10).

In EXP_ELN (Figs. 11d–f), on the other hand, the Gulf-to-U.S. moisture transport is neither increased nor decreased. A weak anomalous upper-level anticyclone is formed (in a long-term and ensemble averaged sense) over North America, and the lower-tropospheric (not shown) and lower-level vertical wind shear values are slightly decreased over the central and eastern United States. In EXP_LAN (Figs. 11a–c), a relatively weak anomalous upper-level cyclone is formed over North America, and thus the lower-tropospheric (not shown)

and lower-level vertical wind shear values are increased in the central and eastern United States. However, the Gulf-to-U.S. moisture transport is not increased.

In summary, these model results support the hypothesis that a positive phase of the TNI with colder than normal SSTs in CP and warmer than normal SSTs in EP enhances the large-scale differential advection in the central and eastern United States and increases the lower-tropospheric and lower-level vertical wind shear values therein, thus providing large-scale atmospheric conditions conducive to intense tornado outbreaks over the United States. However, the model results do not show favorable large-scale atmospheric conditions in

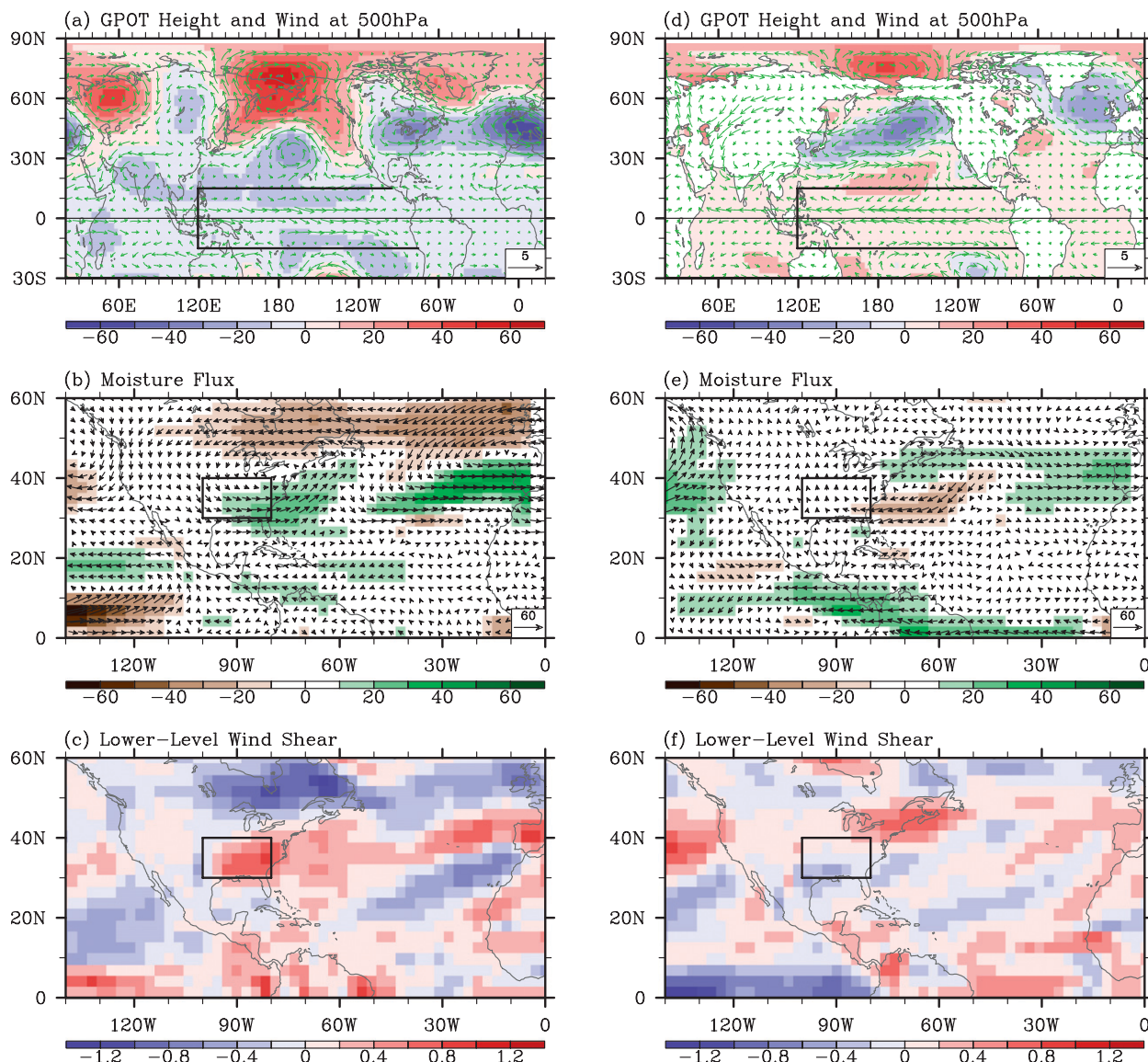


FIG. 11. As in Fig. 10, but for (a)–(c) EXP_LAN – EXP_CLM and (d)–(f) EXP_ELN – EXP_CLM. The values of the 90% confidence interval averaged over the box region are 22 (23) and 0.6 (0.5) for (b) [(e)] and (c) [(f)], respectively.

the central and eastern United States under La Niña and El Niño conditions as long as the SST anomalies in EP are as strong as and of the same sign as the SST anomalies in CP (i.e., neutral phase TNI), consistent with the observations.

6. CP- versus EP-forced teleconnection

The model results strongly suggest that colder than normal SSTs in CP and warmer than normal SSTs in EP may have a constructive influence on the teleconnection pattern that strengthens the large-scale differential advection and lower-tropospheric and lower-level vertical

wind shear values over the central and eastern United States. To better understand how the real atmosphere with moist diabatic processes responds to colder than normal SSTs in CP and warmer than normal SSTs in EP, two sets of additional model experiments (EXP_CPC and EXP_EPW) are performed (Table 4). These two experiments are basically identical to EXP_TNI except that the composite SSTs of the positive phase TNI years are prescribed only in the western and central tropical Pacific region (15°S–15°N, 120°E–110°W) for EXP_CPC and only in the eastern tropical Pacific region (15°S–15°N, 110°W–coast of the Americas) for EXP_EPW. Note that climatological SSTs are prescribed in the eastern Pacific

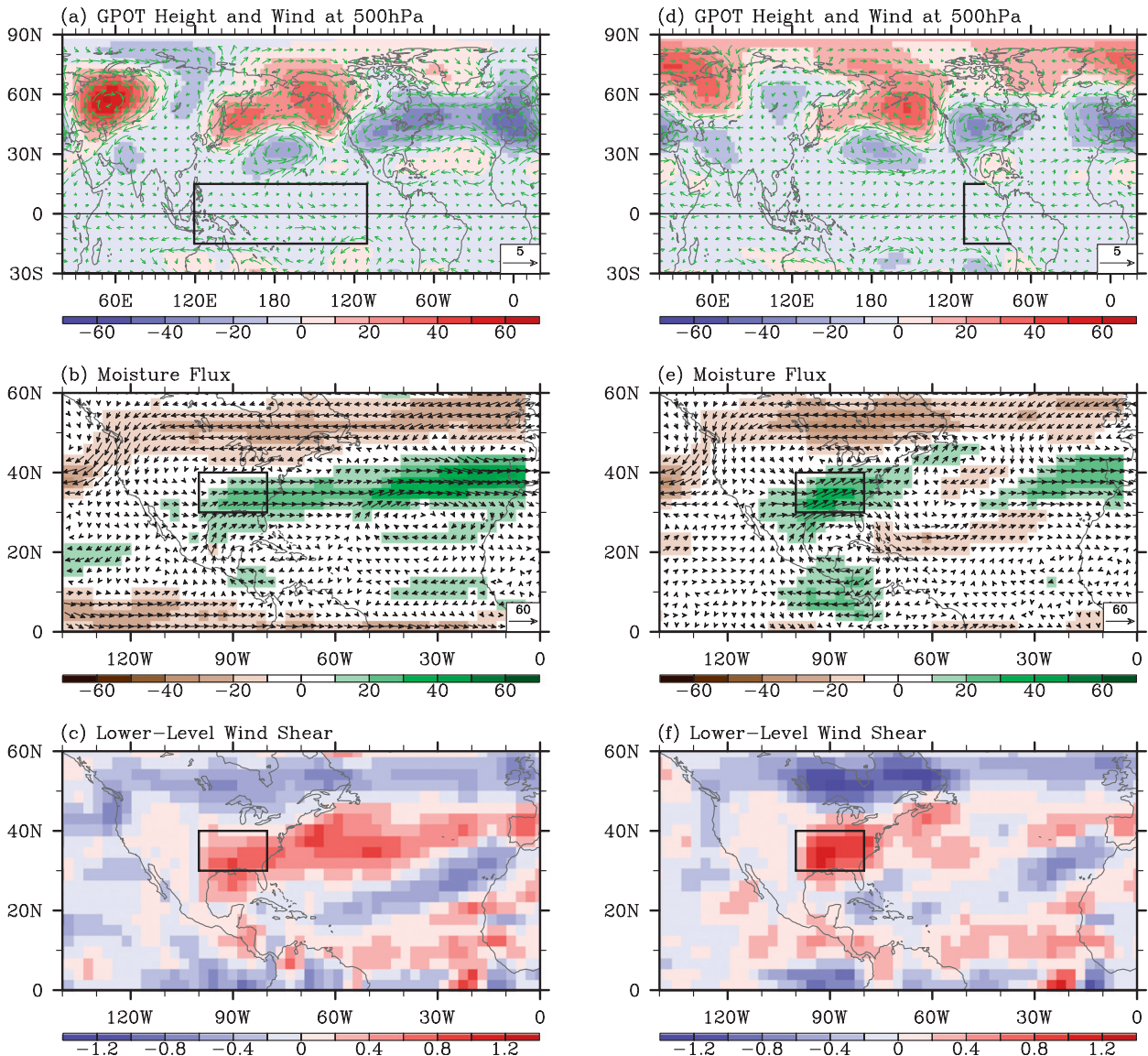


FIG. 12. As in Fig. 10, but for (a)–(c) EXP_CPC – EXP_CLM and (d)–(f) EXP_EPW – EXP_CLM. The values of the 90% confidence interval averaged over the box region are 20 (17) and 0.5 (0.5) for (b) [(e)] and (c) [(f)], respectively.

region (15°S–15°N, 110°W–coast of the Americas) for EXP_CPC and in the western and central tropical Pacific region (15°S–15°N, 120°E–110°W) for EXP_EPW.

In EXP_CPC (Figs. 12a–c), the teleconnection pattern emanating from the tropical Pacific consists of an anticyclone over the Aleutian low in the North Pacific, a cyclone over North America, and an anticyclone over the southeastern U.S. extending to Mesoamerica, consistent with a negative phase PNA-like pattern (Fig. 12a). As expected from the anomalous anticyclonic circulation over the southeastern United States and Mesoamerica, the Gulf-to-U.S. moisture transport is increased in EXP_CPC (Fig. 12b). The lower-tropospheric (not shown) and lower-level

vertical wind shear values are also increased over the central and eastern United States due to the strengthening of the upper-level westerly and lower-level southwesterly winds (Fig. 12c).

Surprisingly, the Rossby wave train forced by warmer than normal SSTs in EP (EXP_EPW) is very similar to that in EXP_CPC (Fig. 12d). Consistently, the Gulf-to-U.S. moisture transport and the lower-tropospheric (not shown) and lower-level vertical wind shear values over the central and eastern United States are also increased in EXP_EPW (Figs. 12e,f) as in EXP_CPC and EXP_TNI. A question arises as to why the teleconnection pattern forced by warmer than normal SSTs in EP is virtually the same as that

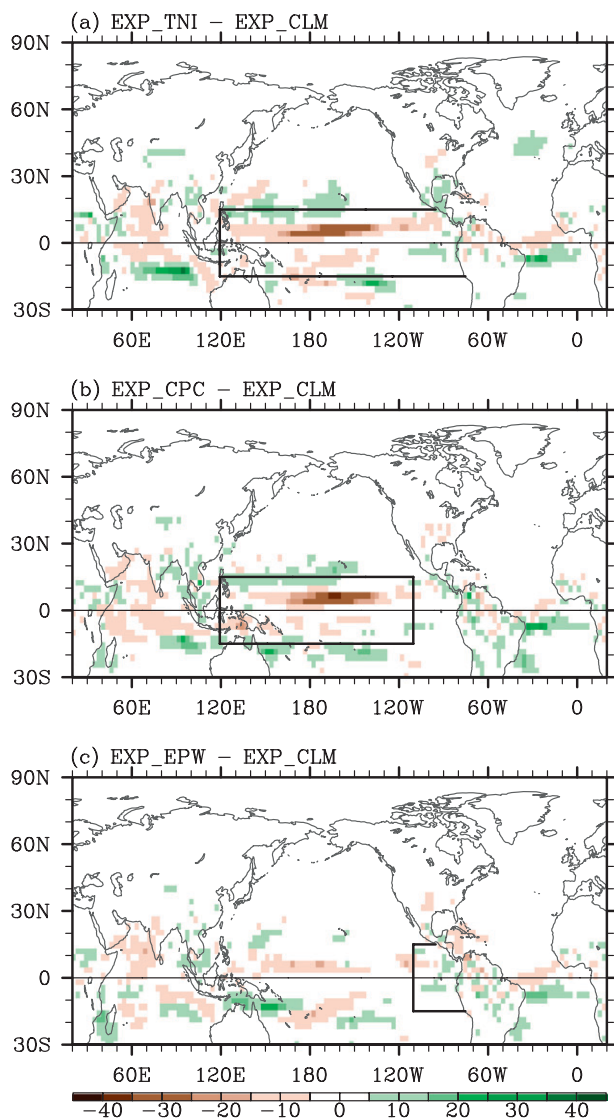


FIG. 13. Simulated anomalous convective precipitation rate in AM obtained from (a) EXP_TNI – EXP_CLM, (b) EXP_CPC – EXP_CLM, and (c) EXP_EPW – EXP_CLM. The unit is mm day^{-1} . Thick black lines indicate the tropical Pacific region where the model SSTs are prescribed. The values of the 90% confidence interval averaged over the tropical Pacific (15°S – 15°N , 120°E –coast of the Americas) are 4.7, 5.2, and 5.1 for (a), (b), and (c), respectively.

forced by colder than normal SSTs in CP. It appears that the Rossby wave train in EXP_EPW is not directly forced from EP. In EXP_EPW, convection is increased locally in EP, but it is decreased in CP as in EXP_CPC (Fig. 13c). This suggests that increased convection in EP associated with the increased local SSTs suppresses convection in CP and that in turn forces a negative phase PNA-like pattern. Therefore, these model results confirm that colder than normal SSTs in CP and warmer than normal SSTs in EP do have constructive influence on the teleconnection pattern

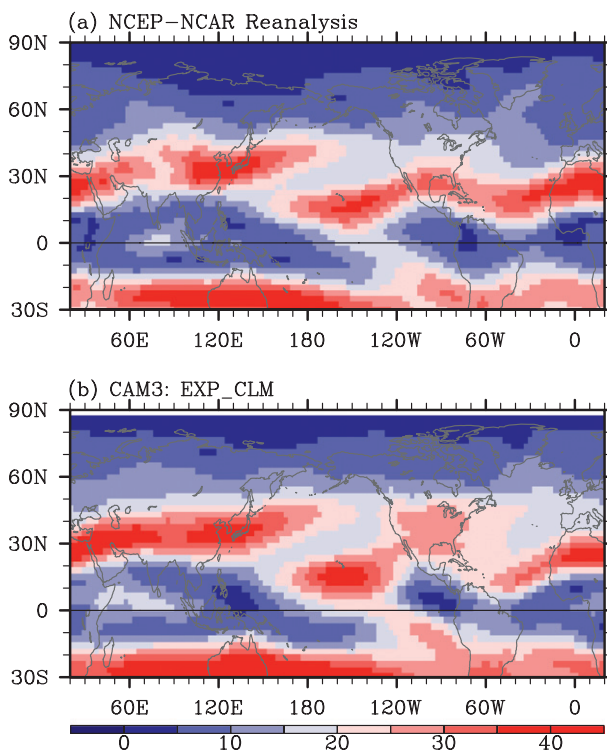


FIG. 14. Background (climatological) vertical wind shear between 200 and 850 hPa in AM obtained from (a) NCEP–NCAR reanalysis, and (b) EXP_CLM. The unit is m s^{-1} .

that strengthens the large-scale differential advection and lower-tropospheric and lower-level vertical wind shear values over the central and eastern United States. The model results also suggest that colder than normal SSTs in CP with neutral SST anomalies in EP or warmer than normal SSTs in EP with neutral SST anomalies in CP can also strengthen the large-scale differential advection and lower-tropospheric and lower-level vertical wind shear values over the east of the Rockies.

An apparently important question is why warmer than normal SSTs in EP does not directly excite a Rossby wave train to the high latitudes. As shown in earlier theoretical studies, the background vertical wind shear is one of the two critical factors required for tropical heating to radiate barotropic teleconnections to the high latitudes (e.g., Kasahara and da Silva Dias 1986; Wang and Xie 1996; Lee et al. 2009). In both observations and EXP_CLM, the background vertical wind shear between 200 and 850 hPa in AM is largest in the central tropical North Pacific and smallest in EP and the western tropical Pacific (WP), providing a potential explanation as to why the Rossby wave train in EXP_EPW is not directly forced in EP (Fig. 14).

Another related and important question is how increased convection in EP associated with the increased local SSTs

suppresses convection in CP remotely. Although answering this question requires a more extensive study, one potential explanation is that the warmer than normal SSTs in EP induces a global average warming of the tropical troposphere via a fast tropical teleconnection mechanism (e.g., Chiang and Sobel 2002), and thus increases atmospheric static stability and decreases convection over CP and other tropical regions of normal SSTs. A similar argument was previously used in Lee et al. (2011) to explain reduced deep convection in the tropical Atlantic in response to warmer than normal SSTs in the tropical Pacific. Another similar argument, but in a different context, is the “upped-ante mechanism,” which is often used to explain anomalous descent motions neighboring warm SST anomalies in the eastern and central Pacific Ocean during El Niño (Su and Neelin 2002; Neelin et al. 2003).

7. Implications for a seasonal outlook for extreme U.S. tornado outbreaks

The conclusion so far is that a positive phase of the TNI, characterized by colder than normal SSTs in CP and warmer than normal SSTs in EP, strengthens the large-scale differential advection and lower-tropospheric and lower-level vertical wind shear values in the central and eastern United States, and thus provides favorable large-scale atmospheric conditions for major tornado outbreaks over the United States. In this sense, a positive phase of the TNI may be an optimal ENSO pattern that increases the chance for major U.S. tornado outbreaks. However, the TNI explains only up to 10% of the total variance in the number of intense U.S. tornadoes in AM. This suggests that intrinsic variability in the atmosphere may overwhelm the positive phase TNI teleconnection pattern over North America as discussed in earlier studies for El Niño teleconnection patterns in the Pacific–North American region (e.g., Hoerling and Kumar 1997). In other words, the predictability of U.S. tornado activity, which can be defined as a ratio of the climate signal (the TNI index in this case) relative to the climate noise, is low.

Nevertheless, seven of the 10 most extreme tornado outbreak years during 1950–2010 including the top three years are characterized by a strongly positive phase of the TNI (Table 2), and the number of intense U.S. tornadoes in AM during the top 10 positive phase TNI years is nearly doubled from that during 10 neutral phase TNI years (Fig. 6). A practical implication of these results is that a seasonal outlook for extreme U.S. tornado outbreaks may be achievable if a seasonal forecasting system has significant skill in predicating the TNI and associated teleconnections to the United States. Obviously, before we can achieve such a goal, there remain many crucial scientific questions to be addressed to refine the predictive

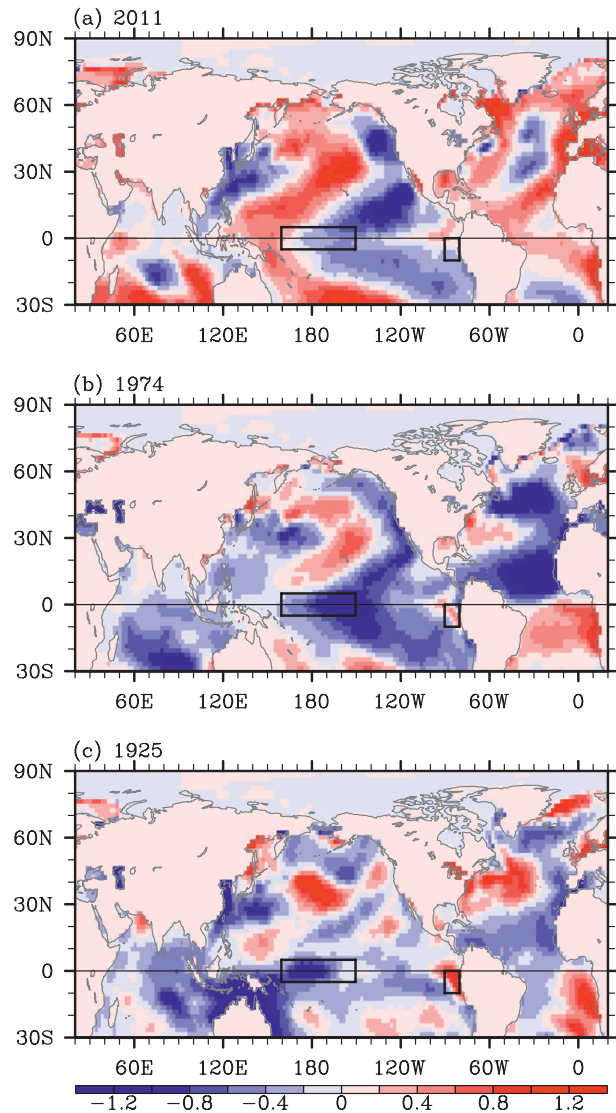


FIG. 15. Anomalous SSTs in AM of three historical U.S. tornado outbreak years, (a) 2011, (b) 1974, and (c) 1925, obtained from ERSST3. The unit is $^{\circ}\text{C}$.

skill provided by the TNI and to explore other long-term climate signals that can provide additional predictability in seasonal and longer time scales.

8. Historical U.S. tornado outbreak years

In terms of annual tornado-related death toll, 2011 was the fourth deadliest tornado year in U.S. history after 1925, 1936, and 1917 (Doswell et al. 2012). 1974 was the 14th, but it was the year in which the largest number of intense tornadoes occurred (Table 2). A positive phase of the TNI prevailed during AM of 2011, 1974, and 1925 with colder than normal SSTs in CP and warmer than normal SSTs in EP (Fig. 15). A positive phase TNI

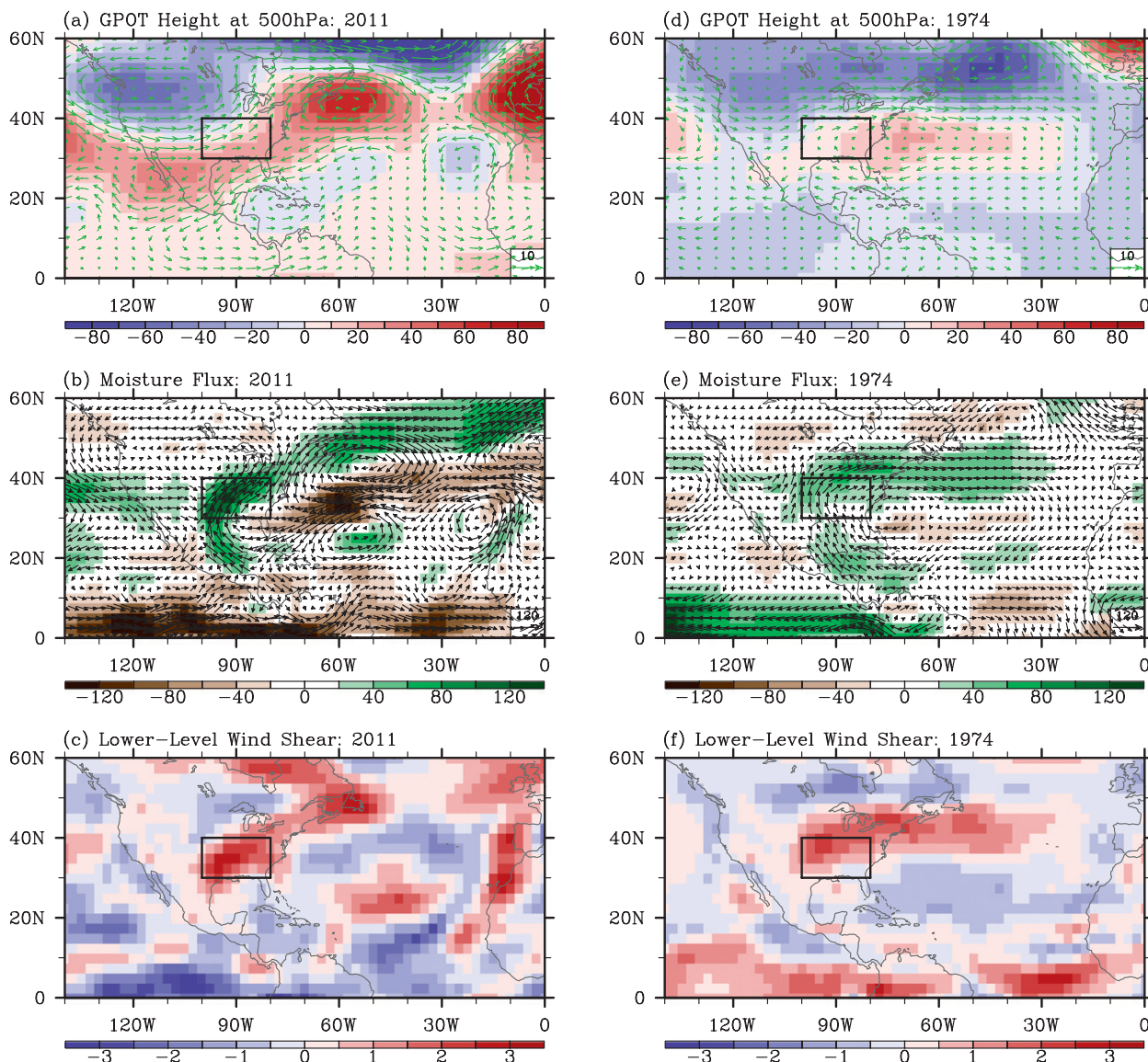


FIG. 16. As in Fig. 4, but for AM of (a)–(c) 2011 and (d)–(f) 1974.

also occurred during AM of the other two historical outbreak years (not shown). In particular, the TNI during AM of 1917 is marked as the strongest TNI during the period of 1854–2011. An important question is whether the series of extreme U.S. tornado outbreaks during AM of 2011 and the other historical U.S. tornado outbreak years can be attributed to the positive phase TNI.

During AM of 2011, an anomalous upper-level cyclone was formed over the northern United States and southern Canada (Fig. 16a), the Gulf-to-US moisture was greatly increased (Fig. 16b), and the lower-tropospheric (not shown) and lower-level vertical wind shear values were increased over the east of the Rockies (Fig. 16c). All of these atmospheric conditions, clearly indicating

the coherent teleconnection response to a positive phase TNI, also prevailed in AM of 1974 (Figs. 16d–f).

To confirm this finding, a set of additional model experiments (EXP_011) is performed by prescribing the SSTs for 2010–11 in the tropical Pacific region while predicting the SSTs outside the tropical Pacific using the slab ocean model (Table 4). The model results are consistent with the observations, although the anomalous Gulf-to-US moisture transport is weaker in the model experiment (not shown). Thus, it is highly likely that the 2011 positive phase TNI event did contribute to the U.S. tornado outbreak in AM of 2011 by enhancing the differential advection and lower-tropospheric and lower-level vertical wind shear values in the central and eastern

United States. A distinctive feature in the 2011 TNI event is warmer than normal SSTs in WP (Fig. 15a). A further experiment (EXP_WPW) suggest that the warmer than normal SSTs in WP indirectly suppress convection in CP and thus work constructively with the colder than normal SSTs in CP to force a strong and persistent negative phase PNA-like pattern (not shown).

9. Discussion

Tornadogenesis is basically a mesoscale problem that requires overlap of very specific and highly localized atmospheric conditions. Therefore, it is not expected to be adequately captured by large-scale and long-term averaged atmospheric processes. In this study, we simply argue that such overlap of the specific conditions for tornadogenesis may occur more frequently on average during a positive phase of the TNI. In addition to the large-scale atmospheric conditions explored in this study, there are other specific atmospheric conditions for tornadogenesis such as lifting condensation level height and convective inhibition. Their associations with the TNI need to be explored in future studies.

It appears that a positive phase of the TNI is associated more with intense tornado activity over the Ohio River valley region, and less with intense tornado activity over the Great Plains (Fig. 6). Recent studies reported that springtime tornado activity over the Ohio River valley region is closely linked to the preferred modes of variability in North American low-level jet (NALLJ) and their shifts in longer time scales (Muñoz and Enfield 2011; Weaver et al. 2012). Future studies need to address the potential linkage among the TNI, the modes of variability in NALLJ, and regional U.S. tornado activity.

One of the caveats in this study, as in any tornado-related climate research, is an artificial inhomogeneity in the tornado database. Eyewitness reports are important sources for tornado count, which can be affected by population growth and migration. Additionally, tornado rating is largely based on the structural damage–wind speed relationship, which can change with time and case by case because every particular tornado–structure interaction is different in detail. For these and other reasons, the historical time series of the tornado database cannot be completely objective or consistent over time (Doswell et al. 2009). In this study, only the intense U.S. tornadoes (F3–F5) are selected and used since intense and long-track tornadoes are less likely to be affected by, although they are not completely free from, such issues in the tornado database. An alternative approach is to develop and use a proxy tornado database, which can be derived from tornadic environmental conditions

in atmospheric reanalysis products. Results from recent studies that used such an approach were very promising (Brooks et al. 2003; Tippett et al. 2012).

Acknowledgments. We thank Harold Brooks, Charles Doswell, Brian Mapes, Gregory Carbin, Kerry Cook, and anonymous reviewers for their thoughtful comments and suggestions. This study was motivated and benefited from interactions with scientists at NOAA NSSL, ESRL, GFDL, CPC, NCDC, and AOML. In particular, we wish to thank Wayne Higgins, Tom Karl, and Marty Hoerling for initiating and leading discussions that motivated this study. This work was supported by grants from the National Oceanic and Atmospheric Administration's Climate Program Office and by grants from the National Science Foundation.

REFERENCES

- Alexander, M., and J. Scott, 2002: The influence of ENSO on air–sea interaction in the Atlantic. *Geophys. Res. Lett.*, **29**, 1701, doi:10.1029/2001GL014347.
- Barnston, A. G., and R. E. Livezey, 1987: Classification, seasonality, and persistence of low-frequency atmospheric circulation patterns. *Mon. Wea. Rev.*, **115**, 1083–1126.
- Brooks, H. E., and C. A. Doswell III, 2001: Some aspects of the international climatology of tornadoes by damage classification. *Atmos. Res.*, **56**, 191–201.
- , J. W. Lee, and J. P. Cravenc, 2003: The spatial distribution of severe thunderstorm and tornado environments from global reanalysis data. *Atmos. Res.*, **67–68**, 73–94.
- Chiang, J. C. H., and A. H. Sobel, 2002: Tropical tropospheric temperature variations caused by ENSO and their influence on the remote tropical climate. *J. Climate*, **15**, 2616–2631.
- Cook, A. R., and J. T. Schaefer, 2008: The relation of El Niño–Southern Oscillation (ENSO) to winter tornado outbreaks. *Mon. Wea. Rev.*, **136**, 3121–3137.
- Doswell, C. A., III, and L. F. Bosart, 2001: Extratropical synoptic-scale processes and severe convection. *Severe Convective Storms, Meteor. Monogr.*, No. 50, Amer. Meteor. Soc. 27–69.
- , H. E. Brooks, and N. Dotzek, 2009: On the implementation of the enhanced Fujita scale in the USA. *Atmos. Res.*, **93**, 554–563, doi:10.1016/j.atmosres.2008.11.003.
- , G. W. Carbin, and H. E. Brooks, 2012: The tornadoes of spring 2011 in the USA: An historical perspective. *Weather*, **67**, 88–94.
- Hoerling, M. P., and A. Kumar, 1997: Why do North American climate anomalies differ from one El Niño event to another? *Geophys. Res. Lett.*, **24**, 1059–1062.
- Horel, J. D., and J. M. Wallace, 1981: Planetary-scale atmospheric phenomena associated with the Southern Oscillation. *Mon. Wea. Rev.*, **109**, 813–829.
- Kasahara, A., and P. L. da Silva Dias, 1986: Response of planetary waves to stationary tropical heating in a global atmosphere with meridional and vertical shear. *J. Atmos. Sci.*, **43**, 1893–1912.
- Lau, K.-M., and H. Lim, 1984: On the dynamics of equatorial forcing of climate teleconnections. *J. Atmos. Sci.*, **41**, 161–176.

- Lee, S.-K., D. B. Enfield, and C. Wang, 2008: Why do some El Niños have no impact on tropical North Atlantic SST? *Geophys. Res. Lett.*, **35**, L16705, doi:10.1029/2008GL034734.
- , C. Wang, and B. E. Mapes, 2009: A simple atmospheric model of the local and teleconnection responses to tropical heating anomalies. *J. Climate*, **22**, 272–284.
- , —, and D. B. Enfield, 2010: On the impact of central Pacific warming events on Atlantic tropical storm activity. *Geophys. Res. Lett.*, **37**, L17702, doi:10.1029/2010GL044459.
- , D. B. Enfield, and C. Wang, 2011: Future impact of differential inter-basin ocean warming on Atlantic hurricanes. *J. Climate*, **24**, 1264–1275.
- Lemon, L. R., and C. A. Doswell III, 1979: Severe thunderstorm evolution and mesocyclone structure as related to tornado-genesis. *Mon. Wea. Rev.*, **107**, 1184–1197.
- Marzban, C., and J. Schaefer, 2001: The correlation between U.S. tornados and Pacific sea surface temperatures. *Mon. Wea. Rev.*, **129**, 884–895.
- Muñoz, E., and D. Enfield, 2011: The boreal spring variability of the Intra-Americas low-level jet and its relation with precipitation and tornadoes in the eastern United States. *Climate Dyn.*, **36**, 247–259, doi:10.1007/s00382-009-0688-3.
- Neelin, J. D., C. Chou, and H. Su, 2003: Tropical drought regions in global warming and El Niño teleconnections. *Geophys. Res. Lett.*, **30**, 2275, doi: 10.1029/2003GL018625.
- Straus, D. M., and J. Shukla, 2002: Does ENSO force the PNA? *J. Climate*, **15**, 2340–2358.
- Su, H., and J. D. Neelin, 2002: Teleconnection mechanisms for tropical Pacific descent anomalies during El Niño. *J. Atmos. Sci.*, **59**, 2694–2712.
- Tippett, M. K., A. H. Sobel, and S. J. Camargo, 2012: Association of U.S. tornado occurrence with monthly environmental parameters. *Geophys. Res. Lett.*, **39**, L02801, doi:10.1029/2011GL050368.
- Trenberth, K. E., and D. P. Stepaniak, 2001: Indices of El Niño evolution. *J. Climate*, **14**, 1697–1701.
- Verbout, S. M., H. E. Brooks, L. M. Leslie, and D. M. Schultz, 2006: Evolution of the U.S. tornado database: 1954–2003. *Wea. Forecasting*, **21**, 86–93.
- Wallace, J. M., and D. S. Gutzler, 1981: Teleconnections in the geopotential height field during the Northern Hemisphere winter. *Mon. Wea. Rev.*, **109**, 784–812.
- Wang, B., and X. Xie, 1996: Low-frequency equatorial waves in vertically sheared zonal flow. Part I: Stable waves. *J. Atmos. Sci.*, **53**, 449–467.
- Weaver, S. J., S. Baxter, and A. Kumar, 2012: Climatic role of North American low-level jets on U.S. regional tornado activity. *J. Climate*, **25**, 6666–6683.
- Whitney, L. F., Jr., and J. E. Miller, 1956: Destabilization by differential advection in the tornado situation 8 June 1953. *Bull. Amer. Meteor. Soc.*, **37**, 224–229.